



An approach to measure trace elements in particles collected on fiber filters using EDXRF

Fatma Öztürk^{a,*}, Abdullah Zararsız^b, Rıdvan Kırmaz^b, Gürdal Tuncel^a

^a Middle East Technical University, Environmental Engineering Department, İnönü Bulvarı, 06531, Ankara, Turkey

^b Turkish Atomic Energy Authority, Sarayköy Nuclear Research and Training Center, 06983, Ankara, Turkey

ARTICLE INFO

Article history:

Received 24 June 2010

Received in revised form

27 September 2010

Accepted 26 October 2010

Available online 2 November 2010

Keywords:

Energy dispersive x-ray fluorescence

Instrumental neutron activation analysis

Whatman-41

Airborne particles

Multi-element analysis

Method development

ABSTRACT

A method developed for analyzes of large number of aerosol samples using Energy Dispersive X-Ray Fluorescence (EDXRF) and its performance were discussed in this manuscript. Atmospheric aerosol samples evaluated in this study were collected on cellulose fiber (Whatman-41) filters, employing a Hi-Vol sampler, at a monitoring station located on the Mediterranean coast of Turkey, between 1993 and 2001. Approximately 1700 samples were collected in this period. Six-hundred of these samples were analyzed by instrumental neutron activation (INAA), and the rest were archived. EDXRF was selected as an analytical technique to analyze 1700 aerosol samples because of its speed and non-destructive nature. However, analysis of aerosol samples collected on fiber filters with a surface technique such as EDXRF was a challenge. Penetration depth calculation performed in this study revealed that EDXRF can obtain information from top 150 μm of our fiber filter material. Calibration of the instrument with currently available thin film standards caused unsatisfactory results since the actual penetration depth of particles into fiber filters were much deeper than 150 μm . A method was developed in this manuscript to analyze fiber filter samples quickly with XRF. Two hundred samples that were analyzed by INAA were divided into two equal batches. One of these batches was used to calibrate the XRF and the second batch was used for verification. The results showed that developed method can be reliably used for routine analysis of fiber samples loaded with ambient aerosol.

© 2010 Elsevier B.V. All rights reserved.

1. Introduction

Inorganic contents of the atmospheric aerosols can be determined by various analytical techniques, some of which require sample preparation prior to analysis whilst some could be employed directly.

XRF, PIXE and INAA are all nuclear analytical techniques used for the assessment of composition of environmental samples. All techniques are multi-elemental and non-destructive in nature and provide simultaneous measurements. These techniques are employed for materials that are hardly taken into solution. Since they do not require chemical destruction prior to analysis, sample contamination is minimized and analytical process accelerates.

Watson et al. [1] reported minimum detection limits attainable for various analytical measurements including INAA, PIXE and XRF for air filter samples. It is obvious from this comparison that number of parameters analyzed in the air filter samples was significantly

higher when the INAA was selected as analytical technique. Biziuk et al. [2] reported that 67 elements from several isotopes can be identified and quantified simultaneously with INAA while number of elements measured was given as 30–40 in Bode [3]. On the other hand, some environmentally important elements such as Cd, Cu, Ni and Pb cannot be measured or hardly measured with INAA [2].

Wang et al. [4] compared ICP-MS with XRF and INAA for the multi-element determinations of airborne particles. Authors concluded that elements such as Cr, As, V and Se cannot be determined using conventional wet chemical analysis since these parameters may loss from the filter matrix through volatilization and can interfere with the spectral analysis. In addition, researchers proposed that XRF can be used as a screening step prior to INAA and ICPMS owing to its non-destructive nature to select the most interesting samples for further analysis. Maenhaut et al. [5] have used INAA as a complement to PIXE to measure additional elements including the light ones (Na, Al), metalloids As, Se, In, Sn and halogen.

The most significant drawback of INAA is that it needs an atomic reactor which increases the cost of analysis. In addition, this technique is not suitable for the determination of some elements with very small or very high period of half-lives [6]. Moreover, measurements can be extended up to one month in order to avoid interferences associated with this technique [2,7]. Consequently,

* Corresponding author at: Abant İzzet Baysal University, Faculty of Engineering and Architecture, Department of Environmental Engineering, Gölköy Campus, 14280, Bolu, Turkey. Tel.: +90 374 254 10 00/2665; fax: +90 374 253 4558.

E-mail address: ozturk.fatma@ibu.edu.tr (F. Öztürk).

INAA is applied less widely than other analytical techniques. In contrast to INAA, analysis time is significantly reduced in XRF and PIXE. It has been reported in the literature that 1 min is enough to obtain 'low-Z' elements concentrations in one PIXE measurement while 30–40 min is required to get the concentrations of 'medium-high Z' elements in one XRF measurement [8].

The detection limits for PIXE and XRF analysis strongly depend on the irradiation time of samples. As the analysis time increases, detection limits can be lowered, which, on the other hand, increases the cost of analysis per sample. In addition, longer irradiation time in case of PIXE results in the loss of elasticity of membrane filters limiting effectively the achievable detection limits. A common disadvantage of XRF and PIXE is that low atomic number elements ($Z < 11$) cannot be accurately measured due to the absorption of the low energy characteristics X-rays by the filter material itself and aerosol deposits. Accurate measurements can be performed when XRF and PIXE are applied to thin film samples in which absorption of X-ray is minimized and correctable [1].

X-ray fluorescence had found wide application in analysis of atmospheric particulate matter, owing to its non-destructive and multi-element nature, but particularly owing to its speed. Analysis of atmospheric aerosols collected on membrane filters is highly reliable since particles are collected on the surface of membrane filters. In contrast to membrane filters, aerosols penetrate deep into filters consisting of irregular array of fibers. Bombardment of these particles with an X-ray beam results in the emission of X-rays from the interiors of the filter. These X-rays are stopped by the particle deposits in the filter media itself resulting in the attenuation of X-ray photons before they reach to filter surface and to detector, resulting in underestimation of elemental concentrations [9]. For this reason, the uncertainty of results when XRF is applied to aerosol samples collected on cellulose or glass fiber filters are noted by various researchers [6,10,11].

The speed and non-destructive nature of XRF was so attractive that people attempted to develop methodologies to be able to use this powerful technique for the analysis of atmospheric particles collected on fiber filters. Rose et al. [12] resuspended NBS (currently NIST) urban particulate SRM (1648) and recollected them on Whatman-41 filters. These filters were then used as standard for analysis of air particulate samples collected on Whatman-41 filters in Brisbane, Australia. Although this was a smart approach, since SRM 1648 was the settling dust collected at an urban area, its size distribution and hence penetration characteristics may not be the same with the particles collected on filters [13].

Chan et al. [13] attempted to develop a methodology that would allow them to analyze aerosol samples collected on Whatman-41 filters using PIXE, which is a surface sensitive technique like XRF. In this study authors collected aerosols on PTFE membrane filters parallel to the Whatman-41 samples. Measured elemental levels from PTFE filters were used to develop the calibration formulae by regression. Calibration equation was then used to measure elemental concentrations on Whatman filters.

Anselmo and Rios [14] attempted to prepare calibration standards by uniformly depositing a standard solution onto glass fiber filters.

Thickness of the sample is very crucial in XRF analysis since it determines the accuracy, detection limits and sensitivity of the measurements. Al-Meray et al. [15] have reported that these figures of merit could be improved particularly for light elements if thin samples were used in XRF analysis.

Identification of pollution source types and their geographical distribution is necessary in order to assess the effectiveness of control strategies taken over air pollutants. Most of the elements measured in the aerosol samples are used as tracers of specific pollution sources. For instance, Cr, Nd, Mg and Cs were found to be the most promising elements to distinguish Saharan dust component

of aerosol from local soil [16]. Biegalski et al. [17] found that Al, Ca, Ce, Fe, Mn, Sc, Ti and V are common crustal markers indicating the impact of earth crust on the chemical composition of collected aerosol samples at the Canadian air sampling stations. In addition to source apportionment studies, identification of chemical composition of atmospheric particles is of particular concern for health related issues. Lead, arsenic, beryllium, cadmium, chromium, copper, selenium and zinc are considered among the potentially toxic elements resulting in the short and long term medical problems [1]. As an example, according to Hirshon et al. [18], elevated ambient air zinc increases pediatric asthma morbidity among the children living in an urban area.

We had 1700 atmospheric particle samples collected onto cellulose fiber filters using high-volume sampler, at a monitoring station on the Mediterranean coast of Turkey. Because of its speed, XRF was the preferred method for trace element analysis in these samples. A method discussed in this manuscript was developed by taking advantage that 200 of these samples were previously analyzed by INAA, which enable us to determine the concentrations of remaining 1500 samples with XRF.

2. Experimental

2.1. Sampling

Detailed information about sample collection and handling can be found elsewhere [16,19], only a brief discussion will be presented here. Daily aerosol samples were collected at a monitoring station located on Turkish Mediterranean coast (30°34'E, 36°47'N) between January 1993 and April 2001. Approximately 1700 aerosol samples were collected in this period. Sierra Andersen Model SAUV-10 H PM10 Hi-Vol air sampler was employed to collect aerosol particles with diameters less than 10 μm on 20 cm \times 28 cm cellulose fiber (Whatman-41) filter. This filter type was selected because of its relatively low background concentrations in terms of elements and compatibility with Hi-Vol sampling [17,20]. Samples were stored in a refrigerator at 4 °C prior to analysis and all sample handling procedures were performed in a Class-100 clean room in the Environmental Engineering Department of Middle East Technical University, Ankara, Turkey. Field and laboratory blanks were also collected and analyzed at regular frequencies.

2.2. Sample preparation

All the collected Whatman-41 filter samples were divided into four equal pieces and different analytical techniques were utilized on each individual part. A total of 600 daily aerosol samples, collected between March 1992 and December 1993, were analyzed in terms of metals by INAA and AAS, major ions (NH_4^+ , SO_4^{2-} , NO_3^- and Cl^-) by ion chromatography and colorimetry and results of the corresponding analysis were published in Güllü et al. [16], Güllü [19], and Güllü et al. [21] where environmental issues (e.g., identification of sources and source regions of aerosols and short and long term variations observed in aerosol composition) mainly discussed in these studies with the exception of basic analytical concepts such as preparation of the samples prior to analysis and operating conditions of the instruments. Last piece of this 600 samples and one piece of the remaining 1100 samples were analyzed by XRF within the content of this study. The XRF analysis was performed on 55 mm diameter filter discs obtained from this last archived piece of sample. These discs were punched out from sample and blank filters using a homemade plexiglass cutter. The important point in this step was to avoid contamination of subsample by the cutter. This was accomplished by designing a cutting device made up of plexiglass, which is practically metal-free. All sample handling, which

Table 1
Optimal excitation conditions used in the analysis of aerosols.

Parameter	Condition number			
	1 (very light elements) 11 < Z < 19	2 (Solids) 19 < Z < 24	3 (Steels) 24 < Z < 26	4 (Medium elements) 26 < Z < 42, Z = 82
Tube voltage (keV)	5	12	15	35
Tube current (mA)	900	900	1000	494
Direct excitation (Ag type of anode)				
Filter thickness	None	Thin Al	Thick Al	Thin Ag
Analysis time (s)	150	100	100	100
Energy range analyzed (keV)	1.0–3.31	3.31–5.41	5.41–6.40	6.40–17.5
Elements analyzed	Mg, Al, Si, P, S, Cl	K, Ca	Ti, Cr, Mn	Fe, Ni, Cu, Zn, Br, Pb

includes punching the disk out of filter, weighting and packaging for transport to XRF laboratory was performed in a clean area, under twice HEPA filtered air.

Possibility of homogeneity problem that could arise due to punching a 55 mm disk from an arbitrary point on a 20 cm × 28 cm filter was tested by punching several disks from the same filter and counting them in XRF for elements with low statistical uncertainty, such as sulfur. Relative standard deviation (RSD) calculated from 5 counting of five filter discs punched from the same filter was not higher than RSD obtained by counting the same disk 5 times, indicating that particles are fairly uniformly distributed across cellulose fiber filters. This conclusion is in agreement with the results of similar tests reported in the literature [22,23].

2.3. Analysis

Fiber filter discs, punched out from filters were analyzed by using an Oxford, model ED2000 Energy Dispersive XRF (EDXRF), at the Ankara Nuclear Research and Training Center of the Turkish Atomic Energy Authority. Samples were loaded to the auto-sampler cassettes, which can accommodate eight samples at once. Spectra were collected using liquid nitrogen cooled Li drifted Si detector, coupled to a DPP Pulse Processor and analyzed by XperEase software. Optimized operating conditions of the instrument, which were used in this study, are given in Table 1. Duration of counting for each excitation condition in Table 1 does not include the dead time of the detector, which approximately equals to the analyze time for each condition. Irradiation of one sample at four different excitation energies took approximately 15 min and one batch of sample containing eight samples was analyzed in a total of 140 min. The K lines of Mg, Al, Si, P, S, Cl, K, Ca, Ti, K- α lines of Cr, Fe, Mn, Ni, Br and Cu, and L- β lines of Pb were used in this study. Pb L- α and As K- α lines were overlapping at 10.5 keV. This spectral interference was overcome by choosing the Pb L- β line at 12.6 keV in the analysis of samples in terms of lead. In this study, we did not interest with the As content of the samples. X-ray spectra of individual runs were illustrated in Fig. 1. With this procedure, on the average, approximately 40 samples were analyzed in a typical working day. The irradiated area for a filter substrate of 47 mm diameter was 17.35 cm².

Instrumental neutron activation analysis was described in detail elsewhere [21] and only a brief discussion is presented in this section. One-eight of the cellulose fiber filters were folded and formed into 2.0-cm diameter pellets under pressure, which are then heat-sealed in acid-washed polyethylene bags. Approximately 10 of these pellets were fit into sample carriers (rabbits) made of high density polyethylene and transferred into the reactor through pneumatic transfer system. Filters were irradiated twice in the 5 MW MITR-II research reactor in a thermal neutron flux of 8×10^{12} n cm⁻² s⁻¹. First irradiation was 1 min and the second one was 12 h long. Irradiated samples were counted three times (5 min and 20 min after 1-min irradiation and 12 h after 12-h irra-

diation). Gamma-ray spectra were collected using high-purity Ge detectors coupled to a 8192-channel pulse-height analyzers (Cannberra, CT). The spectra were analyzed using computer programs (ND 9900 Genie system run on VMS 200, Canberra, CT) to search for the γ -peak(s) of each isotope. NIST Standard Reference Material # 1633 (coal fly ash) was used as a calibration standard in INAA analysis. Accuracy of the analytical technique was checked by analyzing NIST Standard Reference Material # 1571 (orchard leaves) along with samples.

2.4. Quality assurance/quality control

Since large batches of samples were analyzed, it was significant to establish QA/QC protocol necessary to prevent erroneous experimental results systematically or occasionally. The QA/QC protocol followed in this study included proper documentation procedures, calculation of analytical parameters such as precision and detection limits, daily analysis of standard reference filters, re-counting 5% of the samples and analysis of field and laboratory blanks. Proper documentation is an integral part of any QA/QC protocol and applied in this study as well. Daily counting of NIST standard reference filters and reanalysis of selected 5% of the samples were performed to monitor variations in the sensitivity of the instrument in time. If the difference between measured and certified concentrations of elements in NIST SRM is higher than $\pm 10\%$, or if the difference between two counting of reanalyzed samples were higher than 10%, instrument is recalibrated before analyses of samples were resumed.

Precision of the method was tested by 20 repeated counting of a selected sample filter. Relative standard deviations of elements in these 20 counting are given Table 2 in addition to other QA/QC parameters. Relative standard deviations are <5% for S, Ca and Fe and between 5% and 10% for the rest of the measured elements. These RSDs indicate that repeatability of the measurements is not a drawback in analysis of cellulose fiber filters, because expected variability of elemental concentrations in the data set is much higher than the variability due to repeatability of counting.

Field blanks, which are the filters that were loaded to sampler for only 1 min and no air was drawn through the sampler, were collected once in every two weeks. Large number of field blanks was accumulated in 9 years of sampling. Twenty of these field blanks were counted and analyzed in this study. In addition to field blanks two filters, for each batch of 100 filters, were saved and analyzed as laboratory blank. Average sample-to-blank ratios of measured parameters are given in Table 2. It should be noted that values given in the table are average values. Since concentrations of elements in atmosphere can vary by two-to-three orders of magnitude, sample-to-blank ratios that are significantly smaller and higher than the average value presented in the table can be seen for individual samples.

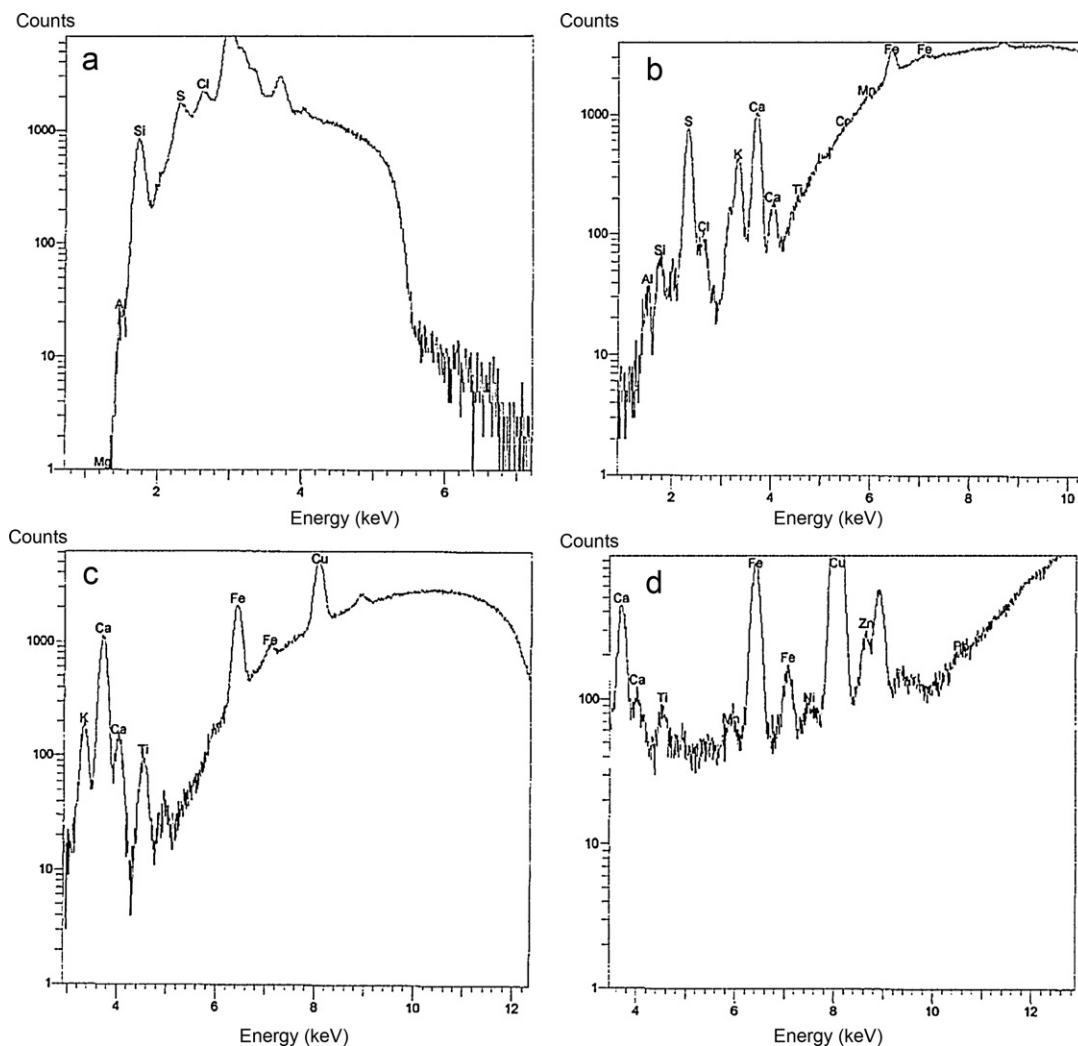


Fig. 1. XRF spectrum of Whatman-41 filter sample using the fixed condition: (a) very light elements, (b) solids, (c) steels, and (d) medium elements.

Magnesium, Cl and Si were not detected in any of the field blanks, indicating that the contribution of blank subtraction on uncertainty in their concentrations is small.

The element with the lowest sample-to-blank ratio is P. High P concentrations observed both in field and laboratory blanks can be

attributed to presence of this element in the filter matrix at considerable amounts. Reliable measurement of P is not possible when cellulose filters are used in sampling. Similar statements are also true for Zn. Average sample-to-blank ratio for Zn is approximately 1.0. Only in 25% of the samples with the highest Zn concentra-

Table 2
Summary of QA/QC parameters in EDXRF analysis.

	SRM 2783 (Avg ± SD)		Sample-to-blank ratio ^b	% RSD
	Certified value (ng) ^a	Measured value (ng)		
Mg	8620 ± 520	7065 ± 390		8.93
Al	23210 ± 530	19580 ± 670	10.6	5.63
Si	58600 ± 1600	59500 ± 1550		6.55
P	–	–	0.99	7.74
S	1050 ± 260	915 ± 165	150	4.63
K	5280 ± 520	4902 ± 570	59	5.71
Ca	13200 ± 1700	14990 ± 1650	30	3.37
Ti	1490 ± 240	1685 ± 270	9.52	7.45
Cr	135 ± 25	146 ± 28	4.21	8.42
Mn	320 ± 12	315 ± 20	1.86	9.26
Fe	26500 ± 1600	30310 ± 1890	24	4.31
Ni	68 ± 12	28.7 ± 15	2.33	8.10
Cu	404 ± 42	277 ± 53	8.62	7.85
Zn	1790 ± 130	1609 ± 123	1.06	6.25
Pb	317 ± 54	320 ± 38		10.0

^a Phosphorus, Cl and Br are not certified in SRM 2783.

^b Magnesium, Si, and Pb were not detected in the field blanks.

Table 3
Detection limits of the measured analytes.

Analyte	DL (μg)	DL ^a (ng m^{-3})	DL ^b (ng cm^{-2})	U (%)
Al	0.62	6.9	36	12
S	1.0	11	58	9.4
Cl	0.31	3.4	18	3.0
K	0.67	7.4	38	6.7
Ca	0.15	1.6	8.5	12
Ti	0.12	1.3	6.8	9.8
Cr	0.088	0.98	5.1	15
Mn	0.091	1.0	5.2	16
Fe	0.21	2.3	12	8.7
Ni	0.068	0.75	3.9	32
Zn	0.060	0.66	3.4	8.2
Br	0.094	1.0	5.4	3.1
Pb	0.11	1.2	6.1	16

^a The average flowrate that passed through the 47 mm diameter filter is about 90.42 m^3 .

^b Concentration is based on 17.35 cm^2 irradiated area for a filter substrate of 47 mm in diameter.

tion blank subtraction was small enough for reliable measurement of Zn concentration. High Zn blanks in cellulose fiber filters were also reported in the literature [10]. Sample-to-blank ratios of the remaining elements were high enough for reliable measurements in most of the collected samples.

NIST standard SRM 2783 (Air Particulate Matter on Filter Media) was repeatedly analyzed to monitor sensitivity and calibration of the instrument. Since SRM 2783 was prepared by collecting $\text{PM}_{2.5}$ particles onto polycarbonate membrane filter, it has not bearing for the analysis of fiber filters, but it shows the general performance of the instrument. Measured concentrations of elements in SRM 2783 and their certified values are given in Table 2. For all the parameters the difference between observed and certified values of elements are smaller than $\pm 20\%$. All the tests performed in section indicates that the XRF instrument used in this study is operating properly and can provide reliable results if appropriate samples are introduced.

Detection limits of measurements for each analyzed parameter were also calculated based on the below equation:

$$C_{DL} = \frac{3}{m} * \sqrt{\frac{N_b}{t}} \quad (1)$$

where C_{DL} is the minimum detectable concentration of analyte (ng), m is the slope of analyte counts–concentration curve (cps/ng) and represents the sensitivity of the instrument, N_b is background concentration (cps), t is the measurement time (s) [24]. Discussion on how to make the conversions from count rates to concentrations is provided in proceeding sections of this manuscript. Detection limit values of measured elements, which were calculated using above procedure are given in Table 3, both in terms of per air volume measured and per irradiated filter surface. As expected, detection limit values of elements in the table decrease with increasing atomic mass. Jenkins [25] has formerly put forward that poorer detection limits of XRF are generally associated with long wavelength extreme of the spectrometer, which corresponds to elements with low atomic number, due to low fluorescence production and increased absorption. Aluminum, chloride, potassium and sulfur are the lightest elements in Table 3 and these elements with the exception of chloride have detection limit values larger than 5 ng m^{-3} . However, relatively poor detection limits of these elements are not a limitation in atmospheric analysis, because their associated concentrations in ambient air are few orders of magnitude higher than these detection limit values. Rest of the elements given in the table have medium to heavy Z values and low–enough detection limits for atmospheric samples.

Relative combined uncertainty of the measured analytes was also tabulated in Table 3. Uncertainty arising from instrument

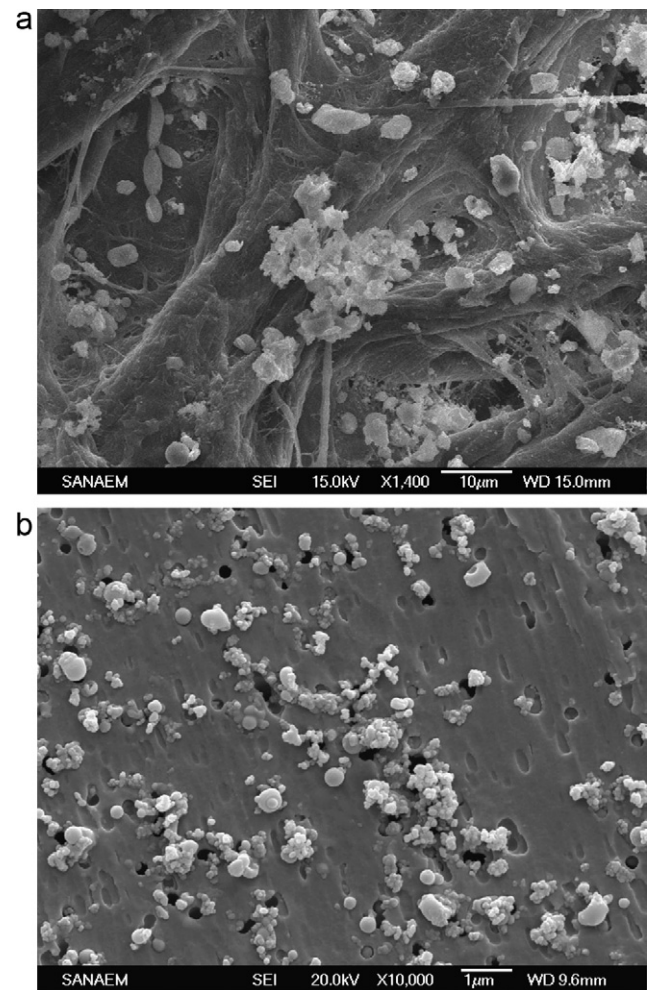


Fig. 2. SEM picture of aerosol loaded cellulose fiber filter; SEM picture of aerosol loaded polycarbonate membrane filter.

stability, counting statistical error, errors that arise from the conversion of the intensities into concentrations (calibration) and uncertainties associated with SRM measurement (accuracy) were considered as the uncertainty sources and propagated together to find relative combined uncertainty. Flow measurement in Hi-Vol sampler and weighing of the filters were not taken into account in uncertainty estimation since these two sources of the uncertainty had already been included in calibration. Highest uncertainty value was obtained for Ni, which can be explained by the lowest accuracy attained in the SRM analysis for this element as provided in Table 2.

3. Results and discussion

Scanning Electron Microscope (SEM) images of particles collected on cellulose-fiber and polycarbonate membrane filters at Antalya and Ankara stations, respectively, are illustrated in Fig. 2a and b. Fig. 2a and b demonstrates very different particle depth profiles on these two types of filters and general incompatibility of cellulose fiber filters for XRF analysis.

As pointed out in previous sections in this manuscript, there are two important sources of uncertainty in XRF analysis on fiber filters. The first and the better appreciated source of uncertainty is the absorption of secondary X-rays emitted from particles penetrated deep in the cellulose matrix by filter material and particle deposits on the filter. [1]. However, primary X-rays have to reach to the particle and excite atoms of elements associated with it prior

Table 4
Specific counts of elements spiked on polyethylene sheets and Whatman filters and that found in 50 samples (cps ng⁻¹).

	Standards spiked on polyethylene sheet			Standards spiked on Whatman filter		Whatman-41 samples
	STM-1	GSP-2	ICP	STM-1	GSP-2	
Mg			0.12 ± 0.39			0.019 ± 0.095
Al	0.91 ± 0.046	0.96 ± 0.079	1.4 ± 0.20	0.12 ± 0.046	0.22 ± 0.013	0.16 ± 0.08
Si	0.46 ± 0.048			0.20 ± 0.014		
S	336 ± 48					11 ± 4
K	5.8 ± 1.4	7.2 ± 2.3	6.7 ± 0.60	2.9 ± 0.90	1.4 ± 0.20	0.50 ± 0.20
Ca	7.9 ± 0.36	4.6 ± 0.66	7.9 ± 1.0	3.2 ± 0.19	4.7 ± 0.59	2.6 ± 0.23
Ti	59 ± 7.2			58 ± 0.6		
Cr	12		11 ± 0.90			
Mn	9.7 ± 4.9	5.9 ± 0.010	15 ± 1.3	27 ± 3.5	5.9 ± 0.030	3.0 ± 1.4
Fe	11 ± 6		20 ± 2	29 ± 4		21 ± 4
Ni			8.2 ± 0.070			8.4 ± 0.60
Cu		160 ± 5	250 ± 10		170 ± 30	
Pb	88 ± 29		29 ± 0.40	13 ± 5.6		12 ± 8.2

to possible absorption of secondary X-rays by the particles. There is a fair chance in fiber filters that the primary X-rays from the source will be attenuated and cannot penetrate the filter deep enough to excite atoms. To test this hypothesis, we calculated penetration depth of primary X-rays into our samples using the following relation, which was derived by the combination of equations discussed by Szilágyi and Hartyáni [10] and Pastuszka et al. [26]:

$$x = \frac{5.38 \times V \times C}{A \times \rho \times \ln\left(\frac{R_0}{R}\right)} \quad (2)$$

In this relation, x is the penetration depth in μm ; V is the sample volume in cubic meters, C is the particle concentration in $\mu\text{g m}^{-3}$, A is loaded filter area in meter square, ρ is the sample density in g cm^{-3} , R_0 and R are the reflectance of blank and loaded filters, respectively.

V in this study is taken as 105 m^3 , which is the average air flow through 55 mm filter disk. Average particle concentration in our study ($2085 \mu\text{g m}^{-3}$) was used for C in the equation. Value used for ρ was calculated by dividing the mass of filter to the irradiated area and average value of the seven filters was taken as 0.0097 g cm^{-3} . Seven reflectance measurements were performed on blank and loaded filters using 8.06 keV Cu K- α source to determine values of R_0 and R . Maximum depth where the primary X-rays can penetrate into Whatman-41 filters was found to be $144 \mu\text{m}$. This value is in agreement with the $100 \mu\text{m}$ penetration depth found in similar filters by Szilágyi and Hartyáni [10], and suggests that the X-ray beam cannot reach to the particles deposited deeper than $150 \mu\text{m}$ of the approximately $300 \mu\text{m}$ -thick filter, which obviously increases uncertainty of the XRF measurements on fiber filters. It should be noted that penetration depth discussed here does not include the uncertainty due to absorption of secondary X-rays by the filter media or by other particles on the filter.

This argument clearly highlights that penetration of elements deep into the fiber filter results in a significant underestimation of elemental concentrations. This is experimentally verified by calculating specific count rate (counts $\text{sec}^{-1} \text{ ng}^{-1}$) for elements spiked onto pre-cleaned polyethylene films, cellulose filters, and for samples collected on cellulose fiber filters. For the spike test, known amounts of elements in a mixed synthetic standard solution (Merck, ICP Multi-Element Standard Solution IV CertiPUR®) as well as digested GSP-2 (Granodiorite Silver Plume, is a medium grained rock containing quartz, plagioclase, microcline, biotite and muscovite, provided by U.S. Geological Survey (USGS)) and STM-1 (Syenite STM-1, a sample of peralkaline nepheline syenite, is provided by USGS) reference materials were spiked onto sets of five pre-cleaned polyethylene sheets and cellulose fiber filter discs in a clean area. Filters were spiked in several spots distributed as smoothly as possible. When droplets spiked to these points are

soaked by the filter they form relatively homogenous distribution of solution. It was actually not attempted to obtain highly homogenous distribution of analyte on the filter, because whole filter surface is exposed to X-ray beam, not a certain fraction of filter (as in microprobe). Because of this, horizontal homogeneity of the analyte is not as important as vertical homogeneity.

Standards spiked onto polyethylene sheets formed a thin layer on the sheet representing conditions similar to aerosol samples collected on membrane filters. Standards spiked onto cellulose fiber filter, on the other hand, approximates the aerosol samples collected onto fiber filters. However, depth profiles of the elements in these spiked fiber filters may not be exactly the same with the depth profiles of elements in atmospheric aerosol samples collected on fiber filters. Polyethylene and cellulose filter discs were then dried under twice HEPA filtered air and counted. Specific count rates of elements (cps ng^{-1}) were calculated by dividing count rates obtained (cps) to the amounts of elements on discs (ng). Specific count rates for the samples collected onto cellulose fiber filters were calculated by dividing the count rates obtained from XRF counting with the ng amounts of elements on the filter measured by INAA (by AAS for Pb and Ni). Results are provided in Table 4.

It is clear from the table that specific count rates of most of the elements measured for polyethylene discs were higher than specific count rates found in cellulose fiber discs and samples. The difference is statistically significant within 95% confidence limit for Mg, Al, S, K, and Ca. Generally speaking, the agreement is better for elements with high atomic weight. Although there were differences between specific count rates of elements spiked onto fiber filters and specific count rates of elements calculated for aerosol samples collected onto fiber filters, these differences were not statistically significant at 95% confidence.

This exercise clearly demonstrated that, the analysis of 1700 aerosol samples collected on cellulose fiber filters with XRF technique was not possible using conventional calibration approaches. A new calibration method was developed that enabled us to analyze these 1700 samples with XRF.

Three quarters of the samples collected in 1993 were analyzed by a combination of INAA, atomic absorption spectrometry (for Pb and Ni) and ion chromatography (IC). There were approximately 200 such samples. These 200 samples were divided into two batches of 100 samples each. One of these batches was used to calibrate the instrument and the second batch was used to check the accuracy of calibration. For calibration, XRF count rates (cps) obtained from samples in the calibration batch were plotted against amounts of elements (ng) measured by INAA (AAS for Ni and Pb). The slope of the regression line was then used as the calibration coefficient to calculate the concentration of elements in the test batch, and in samples for which INAA data were not available. For this, each sample was counted in XRF for about 17 min and

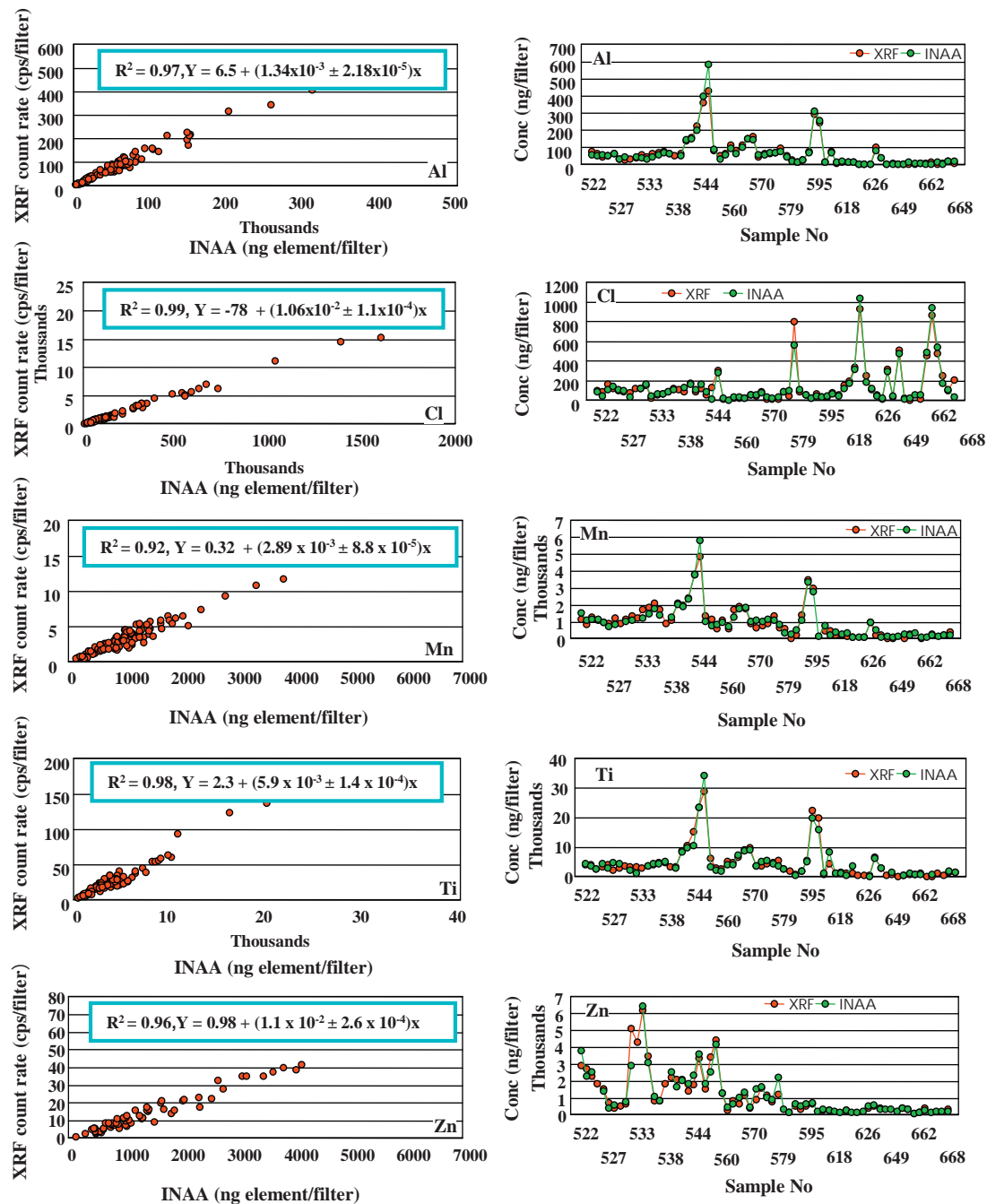


Fig. 3. Scatter plots for calibration of the selected elements.

count rates (cps) of elements obtained was divided by the slope of the regression line acquired from the calibration batch for that particular element. Scatter plots, and regression information for selected elements obtained from calibration batch are given in Fig. 3, together with average concentrations of elements in the test batch, measured by both XRF and INAA. The correlation between specific count rates and ng amounts of elements on filters found by INAA (R^2), were higher than 0.9 for all elements without any exception. Probability of chance correlations ($P(r, N)$) was less than 0.01 (<1%), demonstrating reliability of the slopes used in calibration of the instrument. The R^2 values for elements that were not included in Fig. 3, were 0.92 for Br, 0.98 for Fe, 0.94 for K, 0.90 for Mg, 0.91 for Pb, and 0.92 for S.

The uncertainty of the slope of the regression line of an element is important as it determines the uncertainty of calculated concentration in samples. The uncertainties of the slopes of regression line are also depicted in Fig. 3 for the elements that are shown in the figure. Uncertainty in the slope of the regression line varied between 0.01% for Cl and 4.7% for Mg, indicating that slopes can be safely used to calculate concentrations of elements using count rates obtained from XRF analysis.

Average INAA/XRF concentration ratios of elements for selected samples from the test batch, are depicted in Fig. 4. It is clear from figure that the average ratio was very close to unity implying that methodology developed in this study can be reliably used to convert the intensities into concentrations of aerosol samples.

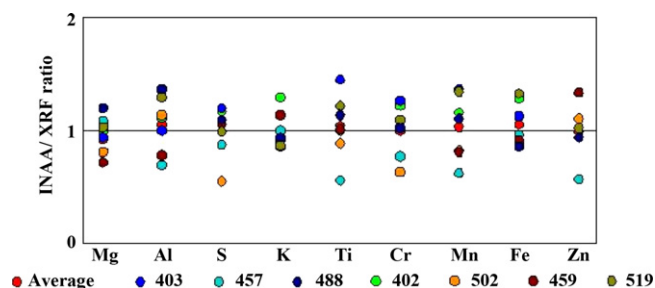


Fig. 4. INAA-to-XRF concentration ratios of elements (XRF data is generated by calibration with the method described in this study).

The calibration approach developed in this study assumes that depth profiles of elements do not change in time at a given sampling point. This assumption needs to be checked, because depth profiles of elements depend on their size distributions in atmosphere, which can change depending on relative abundances of crustal, marine and anthropogenic particles. Relative abundances of these aerosol components can vary with the origin of particles. For example, in the Mediterranean basin, where these samples were collected, transport of air masses from S, SW and SE wind sectors bring coarse crustal and marine particles, whereas transport from W, NW and NE sectors bring fine anthropogenic particles. Unfortunately, there is no data available on how variations in size distribution of particles would affect their depth profiles and hence their count rates for this study. On the other hand, size distributions of trace elements in aerosol samples collected by seven stages Hi-Vol impactor sampler at the same station were evaluated by Kuloğlu et al. [27]. It has been found that mass median diameters (MMD) of crustal elements (such as Al, Ca, Fe, K and Mg) are between 3.0 and 3.5 μm , those of anthropogenic elements (such as Pb, S and Zn) are between 1.01 and 1.25 μm while MMD of elements that have both crustal and anthropogenic sources (such as Cr, Ni, Mn and Ti) is less than 2.0 μm . Based on the MMD of elements, it can be concluded that pollution derived elements are expected to penetrate deepest into the filter material due to their relatively small sizes. Since crustal elements have greater sizes as compared to anthropogenic ones, they retain close to surface of the substrate. Elements with mixed sources probably penetrate much deeper than crustal elements but not than anthropogenic ones.

One-hundred samples used in the calibration batch are distributed uniformly in the year 1993 and represent all likely air mass transport patterns implying that particle size distributions that can be observed in our sampling location are homogenous over the selected samples. The variability in XRF counting statistics due to different depth profiles of particles in different samples contributes to uncertainty of the slope of the regression line of each element. However, since the uncertainties of the slopes of the regression lines of elements, which were discussed in previous paragraphs, are low, we can conclude that the effect of variations in particle size distribution on XRF counting statistics is not large enough to induce a significant uncertainty on the concentrations.

Although the results of our calibration approach were satisfactory in terms of accuracy, it is not practical, because 100 INAA-analyzed samples have to be counted at every time the instrument is calibrated. The method is further modified to avoid this inconvenience. For an element, average specific count rate (cps ng^{-1}) was calculated from 100 samples in the calibration batch and 20 of these samples with specific count rates that are closest to the average were selected. The procedure was repeated for all elements. Finally a batch of 10 samples that are common to as many elements as possible was selected and this batch was used in all further calibrations of the XRF. This approach did not yield 10 point

Table 5

Count intensity normalized to elemental mass for the elements measured in this study, using 100 and 10 sample calibration batches.

	10 Sample counts sec^{-1} $\mu\text{g element}^{-1}$	RSD ^a (%)	100 Sample counts sec^{-1} $\mu\text{g element}^{-1}$	RSD ^a (%)
Mg	0.19 ± 0.021	11.0	0.20 ± 0.033	16.8
Al	1.5 ± 0.20	10.4	1.5 ± 0.20	12.8
S	11 ± 1.1	10.3	13 ± 1.6	12.6
Cl	10 ± 0.81	8.1	9.8 ± 1.6	16.3
K	5.5 ± 1.0	19.8	5.4 ± 1.4	25.9
Ca	4.8 ± 0.25	5.2	4.6 ± 0.47	10.2
Ti	6.9 ± 0.52	7.6	6.9 ± 0.62	9.0
Cr	10 ± 0.81	8.1	9.8 ± 1.6	16.3
Mn	3.1 ± 0.46	14.7	3.2 ± 0.26	8.0
Fe	13 ± 1.0	7.8	13 ± 1.2	9.1
Ni	7.3 ± 0.70	9.7	7.4 ± 0.84	11.3
Zn	10 ± 0.18	17.6	9.8 ± 2.1	21.7
Br	13 ± 1.1	8.9	14 ± 1.4	10.0
Pb	9.5 ± 0.55	5.8	9.8 ± 0.92	9.5

^a Relative standard deviation.

calibration for all elements, because specific count rates of a particular element in this group of 10 samples may not be among the nearest 20 to its average specific count rate. However, all elements did have 6–10 calibration points.

The difference between 100 point and 10 point calibrations was tested by comparing the average specific count rates obtained from each batch. The results are given in Table 5. Ratios of average specific count rates of elements in 100 point and 10 point calibrations varied between 0.89 for Br and 1.18 for S, indicating that results obtained by 100 and 10 point calibrations are not different and 10 point calibration can be routinely used.

4. Conclusions

A relatively simple calibration method was developed for the XRF analysis of 1700 atmospheric aerosol samples collected on Whatman-41 cellulose fiber filters. It is demonstrated that concentrations of elements, particularly those with low atomic weights, are severely under-predicted when the samples were analyzed using regular XRF standards prepared by spiking known amounts of stock solutions on thin mylar or polyethylene films. The under predictions were attributed to penetration of particles bearing elements deep into the fiber filter matrix. A new method of calibration was developed for swift analysis of very large number of samples. Two-hundred samples that were previously analyzed by INAA were used in calibration. These samples were divided into two groups each containing 100 samples. One of the lots was used to calibrate the instrument and the other one was used to check the accuracy of results. The results showed that the method can be reliably used for analysis of aerosol particles collected on fiber filters. Average INAA-to-XRF concentration ratios of elements, which was as high as 7 when the instrument was calibrated with regular XRF procedures varied between 0.8 and 1.2 when the instrument is calibrated with this new method.

Generated huge data set will be treated further by various advanced statistical techniques. For instance, cluster analysis, positive matrix factorization (PMF) and potential source contribution function (PSCF) are the tools that will be employed to identify the sources and source regions of pollutants affecting the chemical composition of Eastern Mediterranean aerosols collected at our station. Since the data generated herein extended over a considerably long period of time, trend analysis techniques will be performed to show whether the pollutants have a well defined trends or not.

References

- [1] J.G. Watson, J.C. Chow, C.A. Frazier, *Elemental Analysis of Airborne Particles, Advances in Environmental, Industrial and Process Control Technologies*, Vol. 1, Gordon and Breach Science Publishers, 1999.
- [2] M. Bizuik, K. Astel, E. Raińska, J. Żukowska, P. Bode, M.V. Frontasyeva, *Anal. Lett.* 43 (2010) 1242–1253.
- [3] P. Bode, in: J. Namiesnik, W. Chrzanowski, P. Zmijewska, T. Hattori (Eds.), *New Horizons and Challenges in Environmental Analysis and Monitoring*, University of Technology Publ., Gdansk, 2003, pp. 1–16.
- [4] C.F. Wang, E.E. Chang, P.C. Chiang, N.K. Aras, *Analyst* 120 (1995) 2521–2527.
- [5] W. Maenhaut, M.T. Fernandez-Jimenez, I. Ratja, P. Artaxo, *Nucl. Instrum. Methods Phys. Res. B* 189 (2002) 243–248.
- [6] O.V. Shuvayeva, K.P. Koutzenogii, V.B. Baryshev, V.I. Rezchikov, A.I. Smirnova, L.D. Ivanova, F.V. Sukchorukov, *Atmos. Res.* 46 (1998) 349–359.
- [7] M. Iwatsuki, T. Kyotani, S. Koshimizu, *Anal. Sci.* 13 (1997) 807–813.
- [8] G. Calzolari, M. Chiari, F. Lucarelli, F. Mazzei, S. Nava, P. Prati, G. Valli, R. Vecchi, *Nucl. Instrum. Methods Phys. Res. B* 266 (2008) 2401–2404.
- [9] O. Haupt, B. Klauke, C. Schaeffer, W. Dannecker, *X-Ray Spectrom.* 24 (5) (1995) 267–275.
- [10] V. Szilágyi, Z. Hartyáni, *Microchem. J.* 79 (2005) 37–41.
- [11] K.P. Koutzenogii, G.A. Kovalskaya, A.I. Smirnova, *Nucl. Instrum. Methods Phys. Res. A* 448 (2000) 434–437.
- [12] H.C. Rose, A. Raftery, W.A. Muller, P.A. Kingston, *Final report on 1985 Brisbane TSP study*, 1986.
- [13] Y.C. Chan, G.H. McTainsh, P.D. Vowles, R.W. Simpson, D.D. Cohen, G.M. Bailey, *Int. J. Environ. Anal. Chem.* 68 (1) (1997) 33–45.
- [14] V.C. Anselmo, J.J. Rios, *Proceedings of the Air Pollution Control Association Annual Meeting*, Vol. 3, 1984, p. 12.
- [15] R. Al-Merey, J. Karajou, H. Issa, *Appl. Radiat. Isot.* 62 (2005) 501–508.
- [16] G. Güllü, İ. Ölmez, G. Tuncel, *J. Radioanal. Nucl. Chem.* 259 (2004) 163–171.
- [17] S.R. Biegalski, S. Landsberger, M.R. Hoff, *J. Air Waste Manage.* 48 (1998) 227–237.
- [18] J.M. Hirshon, M. Shardell, S. Alles, J.L. Powell, K. Squibb, J. Ondov, C.J. Blaisdell, *Environ. Health Perspect.* 116 (2008) 826–831.
- [19] G.H. Güllü, Ph.D. Thesis. Middle East Technical University, 1996.
- [20] J.C. Chow, *J. Air Waste Manage. Assoc.* 45 (1995) 320–382.
- [21] G. Güllü, İ. Ölmez, S. Aygün, G. Tuncel, *J. Geophys. Res.* 103 (D17) (1998) 21943–21954.
- [22] M. Bates, P. Bruno, M. Caputi, M. Caselli, G. de Gennaro, M. Tutino, *Atmos. Environ.* 42 (24) (2008) 6144–6151.
- [23] S.M. Almeida, M.A. Reis, M.C. Freitas, *Nucl. Instrum. Methods Phys. Res. B* 207 (4) (2003) 424–446.
- [24] M.K. Tiwari, A.K. Singh, K.J.S. Sawhney, *Anal. Sci.* 21 (2005) 143–147.
- [25] R. Jenkins, in: R.A. Meyers (Ed.), *Encyclopedia of Analytical Chemistry*, John Wiley & Sons Ltd., Chichester, 2000, pp. 13269–13288.
- [26] J.S. Pastuszka, A. Wawros, E. Talik, U.K.T. Paw, *Sci. Total Environ.* 309 (2003) 237–251.
- [27] E. Kuloğlu, G. Tuncel, *Water Air Soil Poll.* 167 (2005) 221–241.